# Observation of autoionizing transitions $ns^2np^6$-$nsnp^6mp$ in neonlike Mg III and Al IV and argonlike Ca III, Sc IV, Ti V, V VI, Cr VII, and Fe IX

S. O. Kastner, A. M. Crooker,* W. E. Behring, and Leonard Cohen

*Laboratory for Solar Physics and Astrophysics, National Aeronautics and Space Administration Goddard Space Flight Center, Greenbelt, Maryland 20771*

(Received 31 January 1977)

Observations are reported of the autoionizing transitions $2s^22p^6$-$2s2p^6np$ in neonlike Mg III and Al IV and the similar transitions $3s^23p^6$-$3s3p^6np$ in argonlike ions Ca III, Sc IV, Ti V, V VI, Cr VII, and Fe IX. These transitions are present in high-voltage spark spectra as absorption lines of varying width and shape. Both *LS*-allowed and intercombination lines are present. Effective quantum numbers of the upper levels are given, with estimates of the Fano profile parameter $q$. The probable plasma configuration which produces these absorption lines is discussed.

## I. $2s^22p^6(^1S_0)$-$2s2p^6np(^{1,3}P_1)$ TRANSITIONS

In 1967 Codling, Madden, and Ederer[1] reported strong autoionizing transitions in neutral neon in the vicinity of 260 Å, appearing as asymmetrical absorption lines having the well-known Fano profiles associated with levels coupled to a continuum. These lines form a Rydberg series arising from excitation of an inner electron. Only recently has the same Rydberg series been observed in neonlike Mg III by Esteva and Mehlman[2]; still more recently, Lucatorto and McIlrath[3] have observed the series in Na II. An overview of the situation for the neonlike ions is provided by Fig. 1, in which are plotted transition energies $\Delta E$ (in atomic units of $2R$) divided by spectrum number $\zeta$ and referred to the first ionization limit $2s^22p^5(^2P_{3/2})$. The Rydberg series in Ne I, Na II, and Mg III are shown in relation to their ionization limit, which is the $2s2p^6$ level of the next stage of ionization (and hence easily calculated). For Cl VIII and heavier ions of the sequence, we have shown the previously known[4] first members of the series, $2s^22p^6(^1S_0)$-$2s2p^63p(^1P_1)$, which occur as emission lines. From the relative location of the first ionization limit $2s^22p^5$ (the separation between $^2P_{1/2}$ and $^2P_{3/2}$ levels is too small to be shown in Fig. 1) one can deduce the fact that in Al IV the series will usually be seen in absorption, while in P VI, S VII and heavier ions at least the first member may be seen, under suitable conditions, in emission. For Si V, as will be seen below, the precise location of the first member with respect to the first ionization limit remains to be determined.

Weak absorption features in a laser-produced spectrum of aluminum, corresponding to the first two members of the series, have been reported by Carillon *et al.*[5] Valero[6] has commented on the question of establishing the reality of such autoionizing features; more recently (private communication) he believes the features to be present in his own spectra as well as in the spectrum of Carillon *et al.* From our own experience, the particular spatial configuration of the plasma appears to be very important in determining whether the absorptions will be present or not.

We report here a detailed observation of this series of transitions in Al IV in a high-voltage spark spectrum of aluminum obtained as described in a previous publication.[7] From Fig. 1 and also from independent calculations by one of the authors (S.O.K.) to be discussed elsewhere, the wavelengths of the first member of the series were pre-

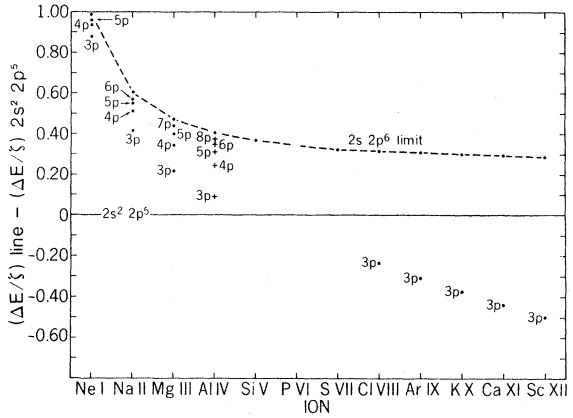


FIG. 1. A plot of members of the Rydberg series $2s^22p^6(^1S_0)$-$2s2p^6np(^1P_1)$ along the Ne I isoelectronic sequence; the ordinate variable is the difference between the value of $\Delta E/\zeta$, for the particular transition, and the value of $\Delta E/\zeta$ for the first series limit $2s^22p^5(^2P)$ ($\Delta E$ is the transition energy in atomic units, $\zeta$ is the spectral number ≡ net charge of core). Points represent existing observations referred to in the text—those for Cl VIII and heavier ions of the sequence are taken from Kelly and Palumbo.[4] Crosses denote the present observations.

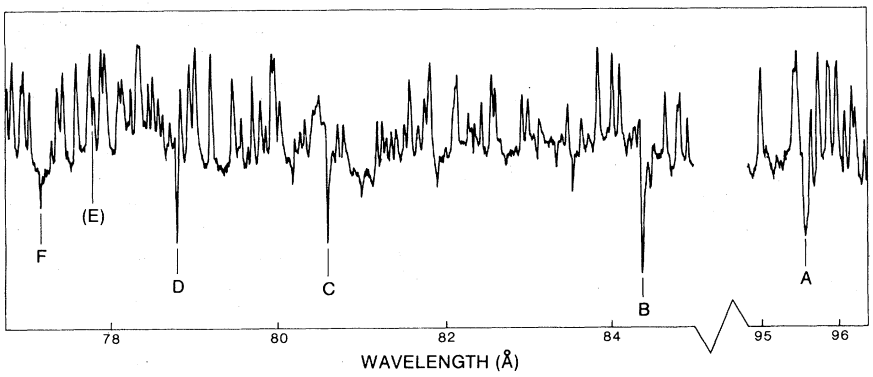


FIG. 2. Observed profiles of the $2s^22p^6$-$2s2p^6np$ series members in aluminum; $A$, $B$, $C$, $D$, $F$ denote $3p$, $4p$, $5p$, $6p$, $8p$, respectively. The $^1S_0-{}^3P_1$ intercombination transitions are present as prominent dips in the long-wavelength wings of the main $^1S_0$-$^1P_1$ profiles, in the cases of members $A$ and $B$.

dicted to be near 95.1, 74.5, and 60.1 Å in Al IV, Si V, P VI, respectively. Examination of our aluminum spectrum showed a number of absorption lines in the spectral range from 95 Å down to the $2s2p^6$ limit at 75.38 Å. Of these, the five features shown in Fig. 2 and listed in Table I form a Rydberg series with smoothly varying effective quantum numbers. In these features, the position of the intensity minimum or "dip" can be most accurately measured, whereas the remainder of the profile is less clearly defined because of the superimposed emission line spectrum—for this reason, the presence of intensity maxima in the continuum associated with the autoionization profiles cannot be definitely ascertained. On the other hand, the superimposed emission lines enable very accurate measurement of the wavelengths of the dips. We have, however, estimated the central wavelengths of each line profile, which are the values given in Table I; for a Fano profile with large value of $|q|$, the central wavelength is the center of the absorption dip. For small $q$ the position of the central wavelength ($E=0$) depends on $q$. Thus, an estimate of $q$ is needed before one can decide where on the profile to measure the wavelength, leading to some uncertainty in wavelengths. We have identified this series of strong absorption lines as $^1S_0$-$^1P_1$, whereas Carillon *et al.*[5] have identified the first three lines of this series as $^1S_0$-$^3P_1$. Our identification gives effective quantum numbers which vary smoothly along the isoelectronic sequence.

The intercombination transitions $2s^22p^6(^1S_0)$-$2s2p^6np(^3P_1)$ are also present in the aluminum spectrum, appearing as narrower profiles of dispersion type superimposed on the longer-wavelength sides of the main $^1S_0$-$^1P_1$ profiles, as can be seen in Fig. 2. These are of special interest in that their presence appears to vary even more with source conditions than the $LS$-allowed lines.

TABLE I. Wavelengths[a] of neonlike transitions $2s^22p^6(^1S_0)$-$2s2p^6np(^1P_1,{}^3P_1)$.

| | Ne I | | Na II | | Mg III | | | Al IV | | |
|---|---|---|---|---|---|---|---|---|---|---|
| Upper level | $\lambda_{CME}$ (Å) | $n^*$ | $\lambda_{LM}$ (Å) | $n^*$ | $\lambda_{EM}$ (Å) | $\lambda$ (Å) | $n^*$ | $\lambda_C$ (Å) | $\lambda$ (Å) | $n^*$ |
| $2s2p^63p(^3P_1)$ | | | | | | | | 95.52 | 95.68 | 2.498 |
| $(^1P_1)$ | 272.21 | 2.155 | 177.24 | 2.319 | 126.50 | 126.49 | 2.430 | 94.48 | 95.56 | 2.503 |
| $2s2p^64p(^3P_1)$ | | | | | | | | 84.37 | 84.48 | 3.506 |
| $(^1P_1)$ | 263.11 | 3.171 | 164.92 | 3.334 | 114.32 | 114.34 | 3.442 | 84.14 | 84.38 | 3.523 |
| $2s2p^65p(^3P_1)$ | | | | | | | | 80.56 | | |
| $(^1P_1)$ | 259.96 | 4.172 | 160.66 | 4.330 | 110.16 | 110.12 | 4.452 | | 80.58 | 4.527 |
| $2s2p^66p(^3P_1)$ | | | | | | | | | | |
| $(^1P_1)$ | 258.48 | 5.172 | 158.67 | 5.304 | 108.08 | | (5.496) | | 78.79 | 5.529 |
| $2s2p^67p(^3P_1)$ | | | | | | | | | | |
| $(^1P_1)$ | 257.68 | 6.150 | 157.55 | 6.281 | 106.92 | 107.05 | 6.438 | | (77.79) | 6.536 |
| $2s2p^68p(^3P_1)$ | | | | | | | | | | |
| $(^1P_1)$ | 257.19 | 7.124 | 156.88 | 7.223 | 106.30 | | (7.576) | | 77.18 | 7.531 |
| $2s2p^6(^2S_{1/2})$ | | | | | | | | | | |
| limit | 255.768 | | 154.836 | | | 104.390 | | | 75.380 | |
| | 390 980 cm$^{-1}$ | | 645 844 cm$^{-1}$ | | | 957 942 cm$^{-1}$ | | | 1 326 610 cm$^{-1}$ | |

[a] $\lambda_{CME}$, $\lambda_{LM}$, $\lambda_{EM}$, and $\lambda_C$ refer, respectively, to wavelengths given by Codling, Madden and Ederer, Ref. 1; Lucatorto and McIlrath, Ref. 3; Esteva and Mehlman, Ref. 2; and Carillon *et al.*, Ref. 5.

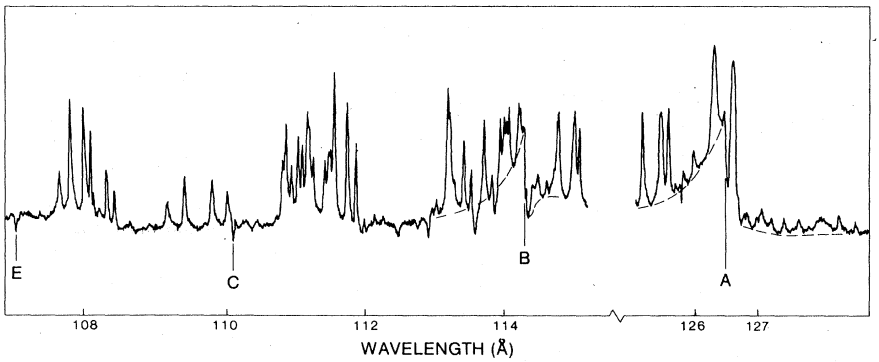


FIG. 3. Observed profiles of the $2s^2 2p^6$-$2s2p^6np$ series members in magnesium; $A$, $B$, $C$, $E$ denote $3p$, $4p$, $5p$, $7p$, respectively. The profile of the first member $3p$ is seen to be extremely wide, though partially obscured by strong emission lines; to shorter wavelengths than the center, the background continuum is raised, while to longer wavelengths the continuum is lowered. The second member $4p$ also has appreciable width as indicated by the background continuum which is sketched in.

The same transitions were found in our magnesium spectrum (strongly in one exposure and weakly in another), at or near the wavelengths reported by Esteva and Mehlman,[2] whose stated accuracy is ± 0.04 Å. Because our wavelengths for the higher members differ somewhat from theirs and appear to yield more smoothly varying effective quantum numbers, they are included in Table I. The spectrum in the vicinity of the individual members of the series is shown in Fig. 3. The existence of the strong absorption "edge" associated with the first member is very pronounced on visual inspection of the plate, extending to more than ± 1 Å from the center of the profile; unfortunately, strong second-order emission lines (2 × 63.295 and 2 × 63.152) of Mg X are seen to be superimposed on the autoionization profile, rendering accurate measurement difficult for this first member.

On both the Mg and the Al plates, emission lines of Mg III and Al IV were present, verifying that these neonlike ions were present. However, a search for the same series of autoionizing transitions in silicon, phosphorus, and sulfur spectra was not successful even though the corresponding neonlike ions were present as shown by their emission lines. Evidently the spark does not always take place in such a way as to produce the spatial plasma configuration needed for the absorption lines to appear, probably a central hotter continuum-emitting region surrounded by a cooler shell in which the neonlike ion is present.

Table I includes the original series found in neon and, for completeness, the new series observed in Na II by Lucatorto and McIlrath.[3] Table I also shows the variation of the effective quantum number for each series member along the isoelectronic sequence.

From the magnesium line profiles illustrated in Fig. 3, the values of the Fano parameter $q$ appear to be of the order of $-1$, implying strong coupling to adjacent continua, while for the aluminum absorption lines in Fig. 2 the values of $q$ appear to be less than $-2$—i.e., have larger negative values—implying less coupling to the adjacent continua. However, such estimates must be regarded as tentative for two reasons; first, as previously mentioned, the existence of the numerous emission lines produces ambiguity in the profile shapes; second, distortion of each profile by relative Doppler shifts between different parts of the spark plasma is almost certainly present, based on our previous experience. (Both of these complicating features are absent in pure absorption experiments on neutral elements, such as those of Codling *et al.*[1])

## II. $3s^2 3p^6$-$3s3p^6 np$ TRANSITIONS

Madden and Codling[8] also observed the analogous series $3s^2 3p^6(^1S_0)$-$3s3p^6 np(^1P_1)$ in neutral argon, but hitherto this series has not been observed in any of the argonlike ions except for Ti V, where the first member has been reported as an emission line by Svensson and Ekberg.[9,10] We have now found absorption lines of the series in ionized calcium, scandium, titanium, vanadium, chromium, and iron. Figure 4, similar to Fig. 1, includes levels from the previously observed argon lines and titanium line and the presently observed lines. Table II gives the wavelengths of the new lines, whose profiles in the cases of titanium and vanadium are simple, sharp absorption dips (implying large absolute values of the Fano parameter $q$) and therefore could be measured very accurately (±0.005 Å). A comparison of the effective quantum numbers of $3s3p^6 np$ in Table II, with those for the related se-

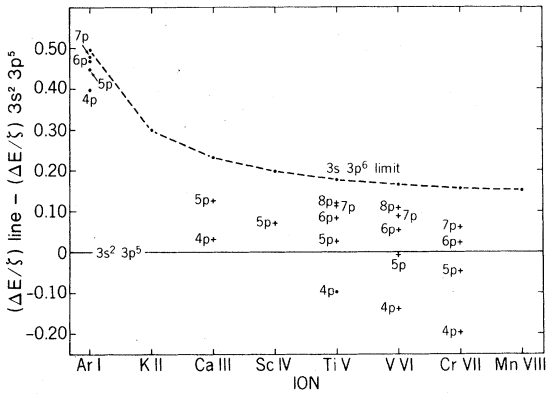


FIG. 4. A plot of members of the Rydberg series $3s^2 3p^6(^1S_0)$-$3s3p^6np(^1P_1)$ along the Ar I isoelectronic sequence, similar to Fig. 1. Again points represent the existing observations of Ne I by Madden and Codling[8] and in Ti V by Ekberg and Svensson, [9] while crosses show the present observations.

ries $3s^2 3p^6 np$ of the next lower stage of ionization, shows expected consistency in that the former are slightly larger by a fairly constant amount due to the decreased screening in $3s3p^6$; in the case of Cr VII and VI, for example, the difference ranges from 0.14 to 0.17. The profiles of the calcium lines are illustrated in Fig. 5; those of the titanium lines in Fig. 6. The first titanium member is seen to be present in this spectrum as a strong absorption line, even though it lies below the series limit.

The intercombination transitions $3s^2 3p^6(^1S_0)$-

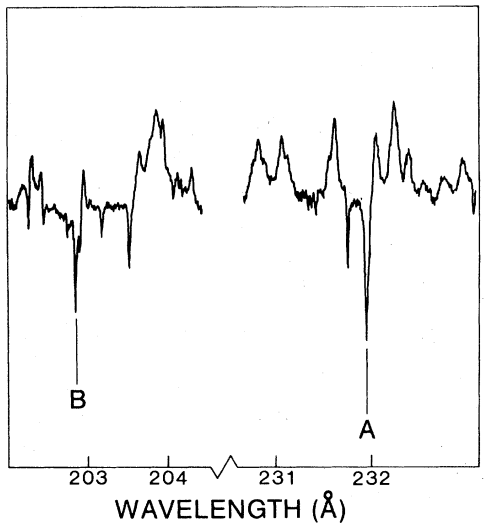


FIG. 5. Observed profiles of $3s^2 3p^6$-$3s3p^6 4p(^1P_1)$ and $3s^2 3p^6$-$3s3p^6 5p(^1P_1)$ in calcium, labeled as $A$ and $B$, respectively.

Table II. Wavelengths (in Å) of argonlike transitions $3p^6(^1S_0)$-$3s3p^6np(^1P_1, ^3P_1)$.

| Upper level | Ar I | | Ca III | | Sc IV | | Ti V | | V VI | | Cr VII | | Fe IX | |
|---|---|---|---|---|---|---|---|---|---|---|---|---|---|---|
| | $\lambda_{MC}$[a] | $n^*$ | λ | $n^*$ | λ | $n^*$ | λ | $n^*$ | $I$[b] | λ | $n^*$ | $I$[b] | λ | $n^*$ | λ | $n^*$ |
| $3s3p^6 4p(^3P_1)$ | | | | | | | 145.354 | 2.977 | 8 | 118.767 | 3.102 | 0.8 | 101.565 | 3.128 | | |
| $3s3p^6 4p(^1P_1)$ | 466.2 | 2.27 | 231.967 | 2.736 | | | 144.551 | 2.996 | 8 | 117.762 | 3.129 | 2 | 100.573 | 3.156 | 72.891 | 3.331 |
| $3s3p^6 5p(^3P_1)$ | | | | | | | 121.138 | 3.994 | 4 | 98.319 | 4.096 | 1 | 81.980 | 4.136 | | |
| $3s3p^6 5p(^1P_1)$ | 443.1 | 3.29 | 202.900 | 3.751 | 153.21 | 3.919 | 120.824 | 4.019 | 4 | 97.932 | 4.131 | 4 | 81.491 | 4.186 | | |
| $3s3p^6 6p(^3P_1)$ | | | | | | | 112.896 | 4.955 | | | | | | | | |
| $3s3p^6 6p(^1P_1)$ | 435.0 | 4.30 | | | | | 112.495 | 5.027 | 6 | 90.700 | 5.131 | 1 | 74.875 | 5.205 | | |
| $3s3p^6 7p(^3P_1)$ | | | | | | | 108.611 | 5.977 | | | | | | | | |
| $3s3p^6 7p(^1P_1)$ | 431.0 | 5.36 | | | | | 108.443 | 6.034 | 3 | 87.106 | 6.147 | | 71.744 | 6.193 | | |
| $3s3p^6 8p(^3P_1)$ | | | | | | | 106.308 | 6.948 | | | | | | | | |
| $3s3p^6 8p(^1P_1)$ | 428.8 | 6.47 | | | | | 106.154 | 7.032 | 1 | 85.071 | 7.159 | | | | | |
| $3s3p^6 9p(^3P_1)$ | | | | | | | 104.732 | 8.107 | | | | | | | | |
| $3s3p^6 9p(^1P_1)$ | 427.5 | 7.57 | | | | | 104.711 | 8.035 | | | | | | | | |
| $3s3p^6 10p(^3P_1)$ | | | | | | | 103.754 | 9.025 | | | | | | | | |
| $3s3p^6 10p(^1P_1)$ | | | | | | | 103.733 | 9.051 | | | | | | | | |
| $3s3p^6 11p(^3P_1)$ | | | | | | | | | | | | | | | | |
| $3s3p^6 11p(^1P_1)$ | | | | | | | 103.059 | 10.046 | | | | | | | | |
| $3s3p^6(^2S_{1/2})$ limit | 424.031 | | 177.603 | | 130.376 | | 100.251 | | | 79.836 | | | 65.187 | | 46.014 | |
| | 235 832 cm$^{-1}$ | | 563 054 cm$^{-1}$ | | 767 012 cm$^{-1}$ | | 997 500 cm$^{-1}$ | | | 1 252 560 cm$^{-1}$ | | | 1 534 040 cm$^{-1}$ | | 2 173 230 | |

[a] $\lambda_{MC}$ refers to wavelengths given by Madden and Codling, Ref. 8.
[b] Relative intensity.

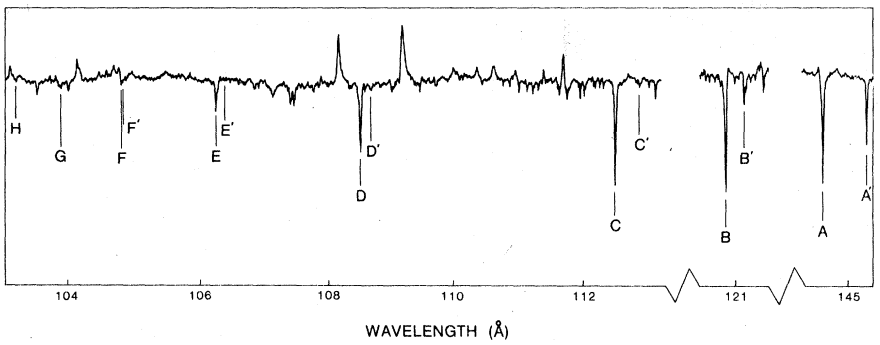


FIG. 6. Observed profiles of $3s^3 3p^6$-$3s3p^6 np$ series members in titanium; $A$, $B$, $C$, $D$, $E$, $F$, $G$, $H$ denote the members $4p(^1P_1)$ to $11p(^1P_1)$, while $A'$, $B'$, $C'$, $D'$, $E'$, $F'$ denote the weaker associated $np(^3P_1)$ transitions.

$3s3p^6 np(^3P_1)$ are also quite intense in the titanium spectrum of Fig. 6, and are similarly relatively intense in vanadium. Their strength relative to the allowed $^1S_0$-$^1P_0$ transition may however depend on the electron density values in the particular spark, judging by their variability from plate to plate. A particularly interesting anomaly is to be noted also in that though the intensities of the $^1S_0$-$^3P_1$ lines were very strong for the first two series members in vanadium, they were not present at all for the third and later members, as recorded in Table II.

We note also that the same wavelengths in V VI which we here classify as $3s^2 3p^6(^1S_0)$-$3s3p^6 4p(^{1,3}P_1)$, namely 117.762 and 118.767 Å, have recently been observed by Ekberg[11] as emission lines (at 117.770 and 118.779 Å) but are ascribed by him to $3p^6(^1S_0)$-$3p^5 5d'[\frac{3}{2}]_1$ and $3p^6(^1S_0)$-$3p^5 5d[\frac{3}{2}]_1$ transitions.

The location of the first member of the series in scandium could not be ascertained because of the presence of several absorption lines in the expected vicinity of 180 Å. These lines remain to be identified.

The profiles of the two calcium lines in Fig. 5 both appear to imply small absolute values of the Fano parameter $q$. Bearing in mind the caution expressed above concerning the interpretation of these lines from a spark source, there may exist a general trend along both isoelectronic sequences such that $q$ takes small absolute values for the early ions of the sequence and larger values for subsequent ions. This would imply that the coupling of the discrete upper levels involved, to the adjacent continua, decreases in general along an isoelectronic sequence.

## III. DISCUSSION

Since in other similar absorption lines in these spectra we consistently observe Doppler shifts corresponding to $v/c = -d\lambda/\lambda \simeq 10^{-4}$, to shorter wavelengths,[12] it is quite possible that the highest temperature plasma occurs in the original pinch, which then produces an expanding and cooling shell of ionic debris; this shell absorbs the continuum—having a broad maximum in the region of 100 Å—emitted by the sustained "fireball" at the center. The oscillatory discharge, with inductance $L = 50$ nH and capacitance $C = 14$ $\mu$F, has a period of about 5 $\mu$sec, so it is probable that the expanding shell does its absorbing within a few centimeters of the spark. We have attempted to correlate the measured shift with the degree of ionization of the absorbing ions, but a significant correlation does not seem to exist.

In our hottest spark pinches, showing excitation corresponding to a temperature near $1 \times 10^7$ K, it is not unusual to find well-developed series of absorption lines, not only Rydberg series from usual levels in ionization stages III to X, but also such autoionizing series as reported here. Valero *et al.*[13] earlier observed absorptions of the former type in laser-generated plasmas. Since the absorption lines are transition from the ground state, they directly establish several important energy levels. Indeed when the highest excitations are achieved, $L$ and $R$ being independently minimized, we observe strongly developed absorption series and even see absorption features associated with emission lines of the 13th stage of ionization.

As indicated above, as well as the autoionizing transitions discussed here, we record absorptions such as $3p^6(^1S_0)$-$3p^5 ns$, $3p^5 nd$. Thus we anticipate, for example in Ti V,[14] a series of $3p^5 ns(^3P_1)$ levels approaching the $^2P_{3/2}$ limit and a series of $3p^5 ns(^1P_1)$ levels approaching the $^2P_{1/2}$ limit. Similarly, from the $3p^5 nd$ configurations we expect similar series $^3P_1$ and $^3D_1$ (in $jK$ notation $d[\frac{1}{2}]_1$ and $d[\frac{3}{2}]_1$) approaching the $^2P_{3/2}$ limit, and a $^1P_1$ series (in $jK$ notation $d'[\frac{3}{2}]_1$) approaching the limit $^2P_{1/2}$. Since the autoionizing transitions also involve $J = 1$ levels $3s3p^6 np(^{1,3}P)$ associated with the limit $3s3p^6(^2S_{1/2})$, there are a total of seven $J = 1$ channels associated with three different limits. The full treatment of the perturbations associated with such a situation is quite complex. A similar three-limit case has recently been treated by Armstrong, Esherick, and Wynne.[15] However, the full multichannel quantum-defect treatment is not needed here because the $n^*$'s here reported vary quite smoothly, which im-

plies that series perturbations are not very important.

As a concluding comment, in most cases it is not possible by visual inspection to distinguish between autoionizing lines that result from transitions involving discrete levels above the ionization limit and those arising from transitions between states below this limit.

ACKNOWLEDGMENTS

We wish to thank C. M. Brown for information concerning the application of the Lu-Fano theory to the multichannel situation mentioned here, and also J. Houston for assistance in the acquisition of spectrograms.

---

*Work supported in part by the National Research Council.

[1]K. Codling, R. P. Madden, and D. L. Ederer, Phys. Rev. 155, 26 (1967).

[2]J. M. Esteva and G. Mehlman, Astrophys. J. 193, 747 (1974).

[3]T. B. Lucatorto and T. J. McIlrath, Phys. Rev. Lett. 37, 428 (1976).

[4]R. L. Kelly and L. J. Palumbo, *Atomic and Ionic Emission Lines Below 2000 Angstroms*, NRL Report No. 7559 (U.S. GPO, Washington, D.C., 1973).

[5]A. Carillon, G. Jamelot, A. Sureau, and P. Jaegle, Phys. Lett. 38A, 91 (1972).

[6]F. P. J. Valero, Appl. Phys. Lett. 25, 64 (1974).

[7]U. Feldman, M. Swartz, and L. Cohen, Rev. Sci. Instr. 38, 1372 (1967).

[8]R. P. Madden and K. Codling, Phys. Rev. Lett. 10, 516 (1963).

[9]L. A. Svensson and J. O. Ekberg, Ark. Fys. 37, 65 (1968).

[10]L. A. Svensson and J. O. Ekberg, Ark. Fys. 40, 145 (1969).

[11]J. O. Ekberg, Phys. Scr. 13, 111 (1976).

[12]W. E. Behring, A. M. Crooker, and F. W. Paul, J. Opt. Soc. Am. 61, 1591 (1971).

[13]F. P. J. Valero, D. Goorvitch, B. S. Fraenkel, and B. Ragent, J. Opt. Soc. Am. 59, 1380 (1969).

[14]L. A. Svensson, Phys. Scr. 13, 235 (1976).

[15]P. Esherick, J. A. Armstrong, R. W. Dreyfus, and J. J. Wynne, Phys. Rev. Lett. 36, 1296 (1976); and J. A. Armstrong, P. Esherick, and J. J. Wynne, Phys. Rev. A 15, 180 (1977).